BİNGÖL UNIVERSITY

Turkish Journal of Nature and Science

e-ISSN: 2149-6366
www.dergipark.gov.tr/tdfd

Research Article

Volume 14, Issue 4, Page 66-84, 2025

Received: 12.08.2025
Accepted: 13.10.2025
Published: 30.12.2025

https://doi.org/10.46810/tdfd.1762609

Task-Specific Airfoil Design for Fixed-Wing UAVs in High-Climb Reconnaissance Missions: A CST and XFOIL-Based Approach

Yunus CELIK[1*]

[1] Sivas University of Science and Technology, Faculty of Aviation and Space Sciences, Department of Aeronautical Engineering, Sivas, Türkiye

**Corresponding author: yunus.celik@sivas.edu.tr*

Abstract

This study presents a systematic airfoil optimisation framework for fixed-wing unmanned aerial vehicles (UAVs) operating in high-climb reconnaissance missions. Emphasizing the climb phase, which is critical for early surveillance and mission efficiency, the approach focuses on optimising aerodynamic performance during this stage. It achieves this by combining Class-Shape Transformation (CST) geometry parameterization with XFOIL-based aerodynamic simulations. Three baseline airfoils (NLF1015, SG6042, TL54) were modified through CST to produce optimised variants. The climb phase was segmented into four altitude-dependent intervals, each analysed using a weighted angle-of-attack (AoA) strategy to reflect realistic aerodynamic demands across varying atmospheric conditions. Simulation results indicate significant improvements in lift-to-drag ratio, climb rate, time-to-altitude, and energy consumption for the optimised designs. The SG6042-derived variant delivered the most balanced performance, with strong lift and stable aerodynamic efficiency. The TL54-based profile achieved the lowest drag, favourable in energy-constrained scenarios. In contrast, the NLF1015-based variant showed limited improvement due to high drag sensitivity at elevated AoA. This study demonstrates the value of phase-specific aerodynamic optimisation in UAV design and supports the use of CST and XFOIL as efficient tools for early-stage performance refinement. The framework offers a foundation for future work involving higher-fidelity CFD models and multi-objective optimisation methods.

Keywords

Phase-specific airfoil optimisation,
Fixed-wing UAV,
Climb-phase UAV performance,
CST method,
XFOIL simulation

BİNGÖL ÜNİVERSİTESİ

Türk Doğa ve Fen Dergisi

e-ISSN: 2149-6366
www.dergipark.gov.tr/tdfd

Araştırma Makalesi

Cilt 14, Sayı 4, Sayfa 66-84, 2025

Alınış: 12.08.2025
Kabul: 13.10.2025
Basım: 30.12.2025
https://doi.org/10.46810/tdfd.1762609

Yüksek Tırmanışlı Keşif Görevlerine Uygun Sabit Kanatlı İHA'lar İçin Göreve Özel Kanat Profili Tasarımı: CST ve XFOIL Tabanlı Bir Yaklaşım

Yunus ÇELİK[1*]

[1] Sivas Bilim ve Teknoloji Üniversitesi, Havacılık ve Uzay Bilimleri Fakültesi, Uçak Mühendisliği Bölümü, Sivas, Türkiye

**Sorumlu yazar: yunus.celik@sivas.edu.tr*

Öz

Bu çalışma, yüksek tırmanışlı keşif görevlerinde görev yapan sabit kanatlı insansız hava araçları (İHA'lar) için sistematik bir kanat profili optimizasyon çerçevesi sunmaktadır. Erken keşif ve görev verimliliği açısından kritik öneme sahip olan tırmanış safhasına odaklanan yaklaşım, Class-Shape Transformation (CST) tabanlı geometrik parametrelendirme ile XFOIL tabanlı aerodinamik simülasyonları birleştirmektedir. Üç referans kanat profili (NLF1015, SG6042, TL54), CST yöntemiyle optimize edilmiş varyantlara dönüştürülmüştür. Tırmanış safhası, irtifaya bağlı olarak dört alt aşamaya ayrılmış ve her biri, farklı atmosfer koşullarında ortaya çıkan gerçekçi aerodinamik talepleri yansıtmak amacıyla ağırlıklı hücum açısı stratejisiyle analiz edilmiştir. Simülasyon sonuçları, optimize edilmiş tasarımlarda taşıma/sürükleme oranı, tırmanış hızı, irtifaya ulaşma süresi ve enerji tüketimi açısından anlamlı iyileşmeler olduğunu göstermektedir. SG6042 temelli varyant, güçlü taşıma kuvveti kabiliyeti ve istikrarlı aerodinamik verimlilik ile en dengeli performansı sergilemiştir. TL54 tabanlı profil, en düşük sürüklemeyi sağlayarak enerji kısıtlı senaryolar için avantaj sunmuştur. Buna karşılık, NLF1015 tabanlı varyant, yüksek hücum açılarında oluşan sürükleme hassasiyeti nedeniyle sınırlı iyileşme göstermiştir. Bu çalışma, İHA tasarımında safhaya özgü aerodinamik optimizasyonun önemini ortaya koymakta ve CST ile XFOIL'in erken tasarım sürecinde etkili araçlar olarak kullanımını desteklemektedir. Sunulan çerçeve, yüksek doğruluklu HAD modelleri ve çok amaçlı optimizasyon yöntemlerini içeren gelecekteki çalışmalar için sağlam bir temel oluşturmaktadır.

Anahtar kelimeler

Fazlara özgü kanat profili optimizasyonu, Sabit Kanatlı İHA, Tırmanış fazında İHA performansı, CST yöntemi, XFOIL simülasyonu

1. INTRODUCTION

In fixed-wing UAV missions, the climb phase represents a critical and energetically demanding segment of the flight envelope [1]. It directly affects time-to-altitude, initial surveillance deployment, and total mission efficiency, factors that are particularly consequential for reconnaissance and time-sensitive operations [2]. The transition from takeoff to cruise requires overcoming gravitational forces while operating in rapidly changing atmospheric conditions, including decreasing air density and pressure, which in turn influence aerodynamic performance and propulsion efficiency [3]. Consequently, optimising aircraft behaviour during this phase has both strategic and operational implications.

From an aerodynamic perspective, the climb phase imposes unique challenges that differ significantly from level or cruise flight. High angles of attack (AoA) are often required to generate sufficient lift during initial ascent, particularly under low Reynolds number conditions that are characteristic of small-to-medium UAVs [4]. These conditions can lead to increased risk of flow separation, reduced control margin, and high drag penalties if the airfoil is not adequately tailored to handle such regimes [5]. Unlike cruise conditions, where flow tends to be more stable and predictable, the climb phase presents a more challenging aerodynamic environment. It demands robust aerodynamic behaviour over a broader range of angles of attack and varying Reynolds numbers due to changes in altitude and airspeed.

In conventional airfoil design, the climb phase is often treated as a secondary consideration, with most optimisation efforts focusing on cruise efficiency or maximum lift conditions for takeoff. However, this traditional approach overlooks the fact that poor aerodynamic efficiency during climb can significantly degrade overall mission performance. For instance, excessive drag during this phase not only increases energy or fuel consumption but also limits payload capacity and reduces the effective operational ceiling [6]. In electrically powered UAVs, where energy budgets are tightly constrained, climb inefficiencies can severely impact range and endurance [7].

Given these challenges, there is a growing recognition of the need to design airfoils specifically optimised for climb performance. For this purpose, this study responds to that need by focusing on the aerodynamic design and phase-specific evaluation of airfoils tailored for the climb envelope. By addressing climb phase criticality with a dedicated optimisation approach, it aims to enhance UAV performance in a mission-relevant context that is too often simplified or overlooked in conventional design frameworks.

1.1. Literature Review

While a wide range of airfoils have been developed and optimised for various applications, such as wind turbine blades [8, 9, 10], the aerodynamic optimisation of airfoils for unmanned aerial vehicles (UAVs) has become a prominent area of research. This is largely driven by the need to enhance performance across diverse mission phases, including climb, cruise, and high-altitude endurance. The following review highlights key research contributions in this domain. Particular emphasis is placed on how tools such as the Class-Shape Transformation (CST) method and XFOIL facilitate targeted airfoil refinement and integration into broader UAV aerodynamic design frameworks.

Rouco et al. [11] presented a comprehensive UAV airfoil optimisation study targeting climb and cruise performance. Using Kulfan's CST method and particle swarm optimisation, they optimised the SD7003 airfoil across multiple mission points; climb, cruise, and takeoff; using XFOIL for aerodynamic evaluations. The CST-based design achieved up to 25% drag reduction in cruise and over 50% in climb, with no lift penalty. The study also compared CST and Bézier parameterizations, showing how the choice of method can bias design outcomes. Their integration of global sensitivity analysis and neural network-driven generative design based on millions of XFOIL runs showed a powerful data-driven approach to aerodynamic optimisation.

Hasan et al. [12] optimised an airfoil for a high-altitude, long-endurance (HALE) solar UAV using Kulfan's CST method and a multi-objective genetic algorithm. Targeting the PHASA-35 platform, their goals were to maximize glide ratio and ensure sufficient lift at high altitude. XFOIL was used for aerodynamic evaluations at low Reynolds numbers, and six CST shape parameters defined the design space. The best-performing airfoil, selected based on CL/CD performance, was later validated with CFD simulations. Although specific gains were not detailed, the study highlighted up to 14% drag reduction in prior work and confirmed that CST-based optimisation with XFOIL is effective for HALE mission profiles.

Nikolaou et al. [13] embedded CST and XFOIL within a multi-fidelity optimisation framework for a small electric UAV wing. In the initial phase, surrogate-assisted optimisation with Gaussian process models and XFOIL was used to identify an airfoil meeting lift requirements for takeoff and climb, while maximizing CL/CD at low Reynolds numbers. This optimised airfoil then informed wing planform design, refined through higher-fidelity tools. The study demonstrates how CST+XFOIL serves not just in isolated airfoil design, but as an effective module within broader UAV design workflows. Notably, the low-fidelity optimised wing closely matched the performance of the high-fidelity version, highlighting XFOIL's reliability for early-stage UAV design.

Other studies reinforce the role of CST and XFOIL in broader design contexts. Benaouali and Kachel [14] applied CST in an MDO framework for general aircraft, treating airfoil optimisation as a key precursor to wing-level design. In more specialised UAV research, CST has also been used to parameterize morphing airfoils, with XFOIL enabling fast evaluation of shape variants before applying high-fidelity methods. Overall, the present study

reflects a shift toward mission-specific airfoil optimisation, where CST and XFOIL facilitate rapid, targeted design aligned with UAV flight profiles.

In summary, CST and XFOIL have consistently enabled high-performance, task-specific airfoil designs for UAVs. As summarized in Table 1, recent studies report 5–15% lift increases and 15–55% drag reductions through shape optimisation, translating to improved climb, endurance, and efficiency. The latest research reflects a mature design approach, combining CST and XFOIL with tools like global sensitivity analysis, surrogate models, and machine learning to balance accuracy with computational efficiency across multi-condition requirements.

Table 1. Summary of airfoil optimisation studies using CST and XFOIL

Authors	Methodology Focus	UAV Application	Key Contributions and Findings
B. Kulfan, J. Bussoletti [15]	CST (Class-Shape Transformation) introduction	General aerodynamic shapes	Introduced the CST method for airfoils/wings; established a versatile, compact parametric representation for airfoil geometry widely adopted in later optimisation studies.
D.A. Masters et al. [16]	CST & other params (PARSEC, B-splines, etc.) – comparative review	General airfoil design	Comprehensive review of seven airfoil parameterization techniques including CST. Provided guidance on each method's strengths; highlighted CST's ability to capture diverse airfoil shapes accurately with few parameters.
D. Anitha et al. [17]	CST + XFOIL (plus PARSEC, splines) with GA/PSO	Conventional airfoil (NACA 4412) – applicable to small UAVs	Integrated CST (and variants) with XFOIL in GA/PSO loops to optimize NACA4412, showing that low-fidelity tools with shape parameterization can yield significant aerodynamic gains over baseline designs.
M.S. Hasan et al. [12]	CST + XFOIL with multi-objective GA	Solar HALE UAV (PHASA-35, high-altitude long-endurance)	Used 6-parameter CST and a two-objective GA with XFOIL to design a high-glide airfoil. Outperformed baselines, improved UAV endurance, and was validated with CFD and wind-tunnel data.
P. Rouco et al. [11]	CST + XFOIL (and Bézier) with PSO; multi-point optimisation	Small fixed-wing UAV (climb & cruise focus)	Optimised a low-Re UAV airfoil for climb and cruise using CST, achieving up to 55% drag reduction. Combined GSA and a neural network trained on XFOIL data for generative, mission-specific design.
E. Nikolaou et al. [13]	CST + XFOIL (low fidelity) with Surrogate Optimisation + high-fidelity CFD	Class I mini-UAV (electric) – full wing design	Carried out a 3-phase UAV design: CST+XFOIL airfoil optimisation, wing planform tuning, and CFD refinement. Low-fidelity results guided efficient wing design and matched CFD, highlighting XFOIL's value in early, mission-specific design.
A. Benaouali, S. Kachel [14]	CST (airfoil) + CFD (wing); wing MDO	General aircraft wing (method applicable to UAVs)	Proposed an MDO framework prioritizing CST-based airfoil optimisation before full wing design, showing that early 2D shape tuning with low-fidelity tools like XFOIL can enhance overall wing performance.

1.2. Scope of Current Study

This study focuses on the aerodynamic optimisation of airfoils specifically for the climb phase of fixed-wing UAV missions that is a segment that poses distinct challenges due to varying altitude, air density, and angle of attack. While many prior studies reviewed above target cruise or generalised performance, climb-specific optimisation remains relatively underexplored despite its critical role in energy efficiency and mission effectiveness, particularly for electric and long-endurance UAVs.

Using CST parameterisation and XFOIL-based simulations, the study evaluates and optimises three UAV-relevant airfoils, NLF1015, SG6042, and TL54, across realistic climb conditions. A key contribution is the segmentation of the climb phase into four altitude bands, allowing for a more accurate representation of the evolving aerodynamic environment. For each region, lift, drag, CL/CD, and derived metrics such as rate, time of climb, and energy consumption are assessed.

Through parametric CST variation and comparative analysis, the study identifies performance gains tied to altitude-specific shape adaptations. These results highlight the operational value of tailoring airfoil geometry to mission segments, reinforcing the role of CST and XFOIL as effective tools for early-stage, mission-driven UAV design.

2. MATERIAL AND METHOD

Designing efficient airfoils for unmanned aerial vehicles (UAVs) engaged in reconnaissance missions demands a balance of high lift (for steep climbs) and low drag (for endurance and cruise efficiency). High-climb reconnaissance UAVs must rapidly reach altitude and loiter for extended periods, which places unique aerodynamic requirements on their wing sections. Traditional airfoil development relied on empirical shaping and wind-tunnel testing, but modern approaches increasingly leverage parametric shape definitions and computational analysis to tailor airfoils to specific mission profiles. In particular, the Class-Shape Transformation (CST) method for geometry parameterization and the use of XFOIL, a rapid panel-method-based solver, have become prevalent in the literature for UAV airfoil optimisation. These tools enable an iterative design loop where airfoil shapes are mathematically defined with a few parameters and quickly analysed for aerodynamic performance, greatly accelerating the exploration of mission-specific designs.

2.1. CST Parametrisation

The Class-Shape Transformation (CST) method provides a powerful mathematical framework for defining and manipulating airfoil geometries through compact and intuitive parameter sets. Originally introduced by Kulfan et al. [15] the CST formulation has become a widely adopted technique in aerodynamic design due to its ability to generate smooth, realistic, and continuously differentiable shapes that satisfy geometric and aerodynamic constraints. It is particularly well-suited for shape optimisation tasks where control over local curvature, thickness distribution, and camber must be achieved with minimal parametric complexity.

In the CST approach, the airfoil surface $y(x)$ is expressed as the product of a class function $C(x)$ and a shape function $S(x)$, augmented by optional trailing edge modifications. The class function defines the general family of shapes (e.g., round nose, sharp trailing edge), while the shape function, constructed from a Bernstein polynomial basis, enables localized control of curvature and slope. The formulation for a surface takes the form:

$$y(x) = C(x) \times S(x) + x\Delta_{zTE} \quad (1)$$

where:

- $C(x) = x^N(1-x)^M$ is the class function,
- $S(x) = \sum_{i=0}^{n} A_i B_i^n(x)$ is the shape function with Bernstein coefficients A_i,
- Δ_{zTE} allows for linear trailing edge offset, typically set to zero for closed TE.

The CST method offers several practical advantages:

- Low dimensionality: With only a few coefficients, a wide range of shapes can be explored without excessive computational overhead [18, 19].
- Smoothness: CST guarantees C1-continuity and geometric smoothness, critical for numerical stability in simulation tools like XFOIL [20, 21].
- Scalability: The method readily extends to 3D wing surfaces and inverse design workflows, enabling future integration with high-fidelity CFD-based optimisation pipelines [22, 23].
-

Ultimately, the CST parametrisation enabled the creation of refined, mission-tailored airfoil geometries with enhanced aerodynamic performance characteristics for each phase of the UAV climb profile. These optimised shapes form the core dataset for subsequent aerodynamic and mission-level analysis.

2.2. XFOIL Simulation Setup

XFOIL is an open-source aerodynamic analysis tool developed by Mark Drela [24], widely used for the evaluation of two-dimensional subsonic airfoils operating in low-to-moderate Reynolds number regimes. It couples an inviscid panel method for potential flow with a boundary layer integral method for viscous flow modelling, enabling the prediction of lift, drag, and moment coefficients over a broad range of angle of attack (AoA). Although originally developed for airfoil analysis in gliders and light aircraft, XFOIL remains highly relevant for small-scale UAV applications due to its computational efficiency and acceptable accuracy in pre-stall conditions [25, 26].

In this study, XFOIL v6.99 was employed to perform steady-state aerodynamic analysis for all baseline and CST-generated airfoil variants. Each profile was simulated across a wide AoA range. It allows to adequately capturing of aerodynamic performance trends, particularly near stall and transitional flow regions where non-linear effects are pronounced. The AoA bounds were selected to encompass all operational conditions encountered throughout the climb phase, based on both mission data and historical UAV performance studies.

While XFOIL is limited by its inability to resolve fully separated or unsteady flow phenomena, and by its inherently 2D flow assumptions, its low computational cost and adequate accuracy in attached flow regions make it highly effective for early-stage optimisation and sensitivity studies. Its use in this study enables the evaluation of hundreds of airfoil variants in a manner that would be infeasible with high-fidelity CFD alone, thus bridging the gap between conceptual design and advanced analysis.

The CST-based geometry generation and the subsequent aerodynamic simulations using XFOIL were fully integrated into a unified Python workflow (see Appendix A). This automated pipeline enabled the systematic creation of airfoil variants through controlled CST coefficient perturbations, followed by batch simulation of aerodynamic performance metrics (e.g., CL, CD, and CL/CD) across relevant Reynolds numbers and angles of attack. The integration significantly accelerated the design space exploration process, ensured consistency between geometry and simulation phases, and allowed efficient post-processing and comparison of hundreds of airfoil configurations under mission-specific climb conditions.

2.3. Mission Profile and Problem Definition

The HCUAV RX-1, which is shown in Figure 1, was selected as the reference configuration due to its well-defined, multi-phase vertical climb trajectory extending from ground level to operational reconnaissance altitude (~2000 m) [27]. The RX-1's mission architecture reflects real-world UAV operational demands, where rapid and efficient altitude gain is critical for early mission execution and surveillance coverage. Moreover, the HCUAV configuration has been extensively validated using high-fidelity CFD analyses, which supports the credibility and relevance of using this profile to assess airfoil performance in each climb phase. This makes the RX-1 climb profile an ideal benchmark for evaluating and optimising airfoil geometries based on time to climb and aerodynamic efficiency across realistic operating envelopes.

Figure 1. 3D model of the reference fixed-wing UAV [27] used for climb performance analysis

The Figure 2 shows a fixed-wing UAV's mission profile from ground level to cruise altitude. It begins with warmup and takeoff (Point 0 to 1), followed by a climb phase (Point 1 to 2) reaching 2000 meters, and transitions into cruise flight. This schematic highlights the climb segment as a key focus for performance evaluation. For this reason, in the presents study, the climb phase (Point 1 to Point 2, up to 2000 meters) will be specifically investigated to evaluate and compare the aerodynamic performance of selected airfoils and their different variations under varying altitude conditions.

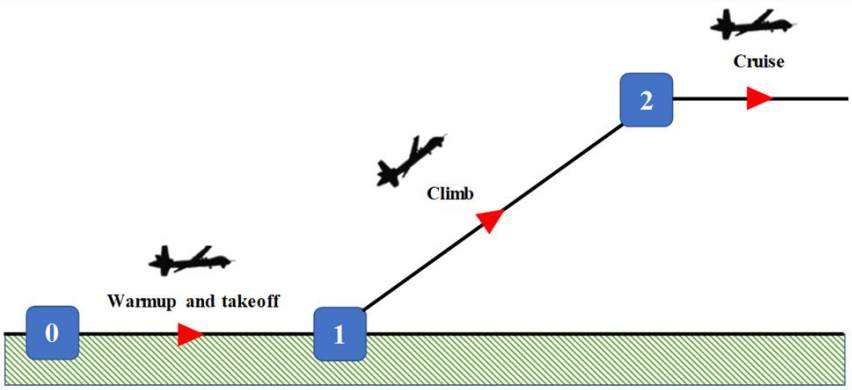

Figure 2. UAV mission profile highlighting the climb segment from takeoff to cruise altitude

The airfoils NLF105, SG6042, and TL54 were selected based on their proven performance in low Reynolds number regimes, climb efficiency, and relevance to UAV applications. NLF105, adopted from the reference study by Panagiotou & Yakinthos [27], is optimised for natural laminar flow and high-lift characteristics. SG6042 is known for its high lift generation at moderate Reynolds numbers, making it suitable for efficient ascent [28]. TL54, on the other hand, is designed for steep climb scenarios, offering strong aerodynamic stability and lift at low speeds [29]. These three airfoils, with their distinct aerodynamic behaviours, provide a robust basis for comparative analysis across the segmented climb phases of the UAV mission.

2.4. Breakdown of Climb Phase

In this study, the climb phase from Point 1 to Point 2 (ground level to 2000 meters) is subdivided into four distinct altitude bands, each referred to as a separate phase. This segmentation allows for a more precise analysis of aerodynamic performance under realistic atmospheric and flight conditions. The climb phase is divided into four altitude segments: Phase 1 spans from 0 to 200 meters, Phase 2 from 200 to 800 meters, Phase 3 from 800 to 1500 meters, and Phase 4 from 1500 to 2000 meters.

Each phase reflects a specific change in air density, Reynolds number, and flow regime, which influence the lift and drag characteristics of the airfoil. This structured approach ensures that airfoil performance is evaluated not as a single climb segment but across multiple altitude-dependent conditions, enabling selection of the most suitable airfoil variations for each part of the ascent.

The key aerodynamic parameters corresponding to each of these four phases are summarised in Table 2. The table presents the average altitude, speed, Reynolds number, air density, Mach number, and significant angle of attack (AoA) ranges for each phase. These parameters were derived based on estimated flight conditions and are essential for understanding the aerodynamic behaviour of the airfoil during ascent. The variation in Reynolds number and Mach number across phases reflects the changing aerodynamic regime, while shifts in density and AoA ranges illustrate the evolving lift requirements. By analysing these parameters phase-by-phase, the study captures the nuanced effects of altitude on aerodynamic performance, supporting informed airfoil selection and optimisation.

Table 2. Summary of key aerodynamic parameters for each climb phase

Phase No.	Description	Estimated Altitude (m)	Average Altitude (m)	Average Speed (m/s)	Average Reynolds Number	Average Density	Average Mach Number	Significant AoA Range (°)
1	Takeoff Transition	0 – 200	100	22.5	1330000	1.2133	0.066	10 – 16
2	Initial Climb	200 – 800	500	27.5	1550000	1.1672	0.081	8 – 14
3	Steady Climb	800 – 1500	1150	32.5	1690000	1.0953	0.091	6 – 12
4	Pre-Cruise Levelling	1500 – 2000	1750	37	1820000	1.032	0.111	4 – 10

3. RESULTS AND DISCUSSION

3.1. Model Validation

For the validation part of the present study, a reference case from the literature Panagiotou & Yakinthos [27] was selected. The validation was performed under flight conditions corresponding to an altitude of 2000 meters, an incoming flow velocity of 38.89 m/s, and a Reynolds number of 1.9×10^6. The NLF1015 airfoil profile was employed as the test geometry for this validation effort.

Figure 3 presents a comparative analysis of lift coefficient (CL) as a function of angle of attack (AoA), ranging from −8° to 20°, using two datasets: reference CFD results (denoted as "CFD Results Panagiotou & Yakinthos [27]") and the current XFOIL model predictions. Both datasets exhibit a generally linear increase in lift with increasing angle of attack up to approximately 16°, after which the lift tends to plateau, indicating the onset of stall. Across the entire pre-stall range, the XFOIL model consistently predicts higher lift coefficients than the CFD results, with the largest overprediction occurring near AoA=0° to 8°. The stall onset appears to be captured reasonably well in both datasets, with both curves showing a levelling-off beyond AoA=16°. At higher angles, the lift values predicted by XFOIL begin to converge with the CFD data, though a slight underprediction can be observed near the maximum CL.

In summary, while XFOIL provides a qualitatively consistent trend and acceptable estimates for preliminary design purposes, it systematically overpredicts lift in the linear range and may not fully capture nonlinear effects near stall. However, given its reasonable agreement with reference data and its computational efficiency, the validated XFOIL-based model is deemed sufficiently accurate to be employed in the subsequent analyses conducted in the present study.

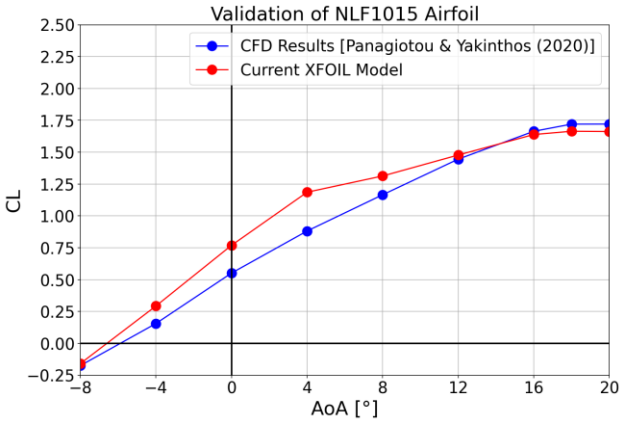

Figure 3. Validation of XFOIL model against reference CFD results [27] for NLF1015

3.2. Airfoil Geometry Modifications

To explore the aerodynamic sensitivity and potential performance improvements of selected airfoils, a systematic shape variation procedure was employed using the Class-Shape Transformation (CST) method. For each airfoil surface (suction and pressure), 9 CST coefficients were utilized to accurately represent the original geometry. A total of 60 geometric variations were generated per airfoil by perturbing the CST coefficients within a controlled range (variation ratio of 0.25), offering a balanced trade-off between design diversity and computational efficiency for the XFOIL-based optimisation framework. The selected CST coefficient values, number of variants, and variation ratio can be further expanded depending on the availability of computational resources. However, this present parametric approach ensured sufficient geometric diversity while maintaining realistic and aerodynamically feasible profiles [30]. The generated variants were then evaluated, and the best-performing shape in terms of aerodynamic metrics (CL/CD ratio) was identified for each baseline airfoil. Comparative plots of the original and best variation airfoils are presented in Figure 4, highlighting the subtle but effective modifications introduced through the CST-based variation process.

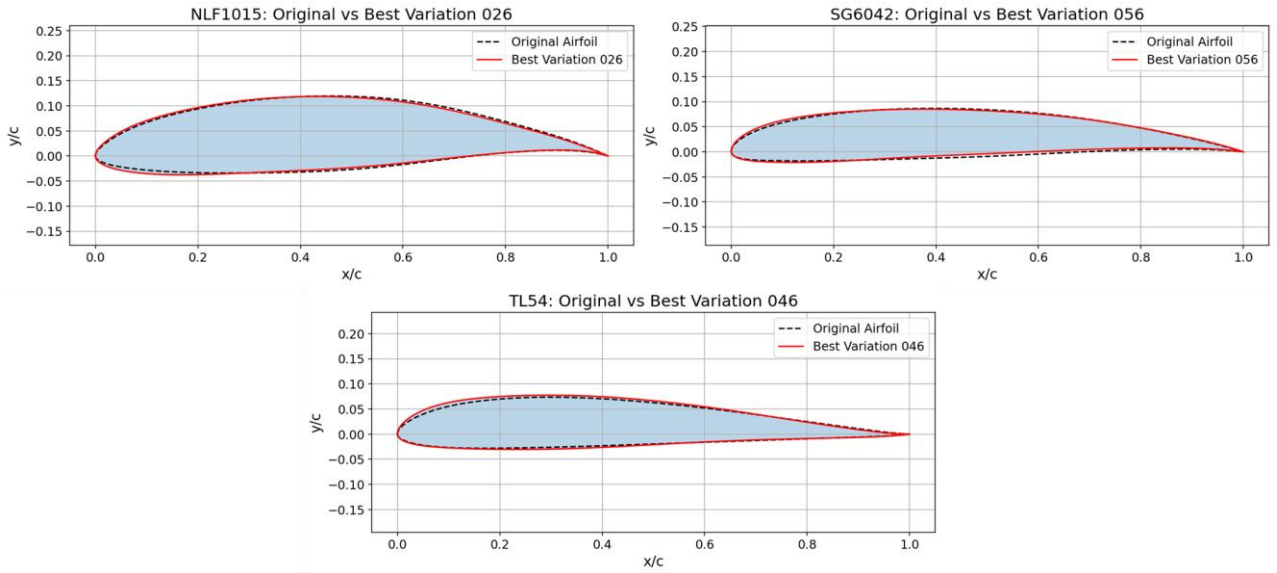

Figure 4. CST-based geometry variations of baseline airfoils

3.3. Aerodynamic Performance per Phase

3.3.1. Angle of attack weighting strategy

Each angle of attack (AoA) was assigned a weighting factor that represents its relative importance within the operational profile, ensuring a realistic and phase-specific assessment of aerodynamic performance during the climb, as shown in the Table 3. These weights were determined based on a set of well-defined aerodynamic and functional criteria, rather than treating all AoA values as equally significant.

The weighting strategy employed in this study is structured around three fundamental guiding principles to ensure both aerodynamic realism and operational relevance. First, higher weights (typically between 2.5 and 3.0) were assigned to angles of attack (AoAs) that exhibit superior aerodynamic efficiency, particularly those corresponding to maximum lift-to-drag (CL/CD) ratios. These conditions are critical for optimising climb performance, enhancing overall lift capability, and reducing energy or fuel consumption during sustained ascent. Second, moderate weights (ranging from 1.5 to 2.5) were applied to AoAs that represent the typical operating range of the airfoil. These conditions are characterised by stable lift generation, predictable aerodynamic response, and smooth phase transitions. Because such AoAs are maintained for longer durations throughout the climb phase, they play a central role in determining the aircraft's overall performance stability and controllability. Finally, lower weights (between 1.0 and 1.5) were reserved for AoAs that are only momentarily encountered or are associated with higher aerodynamic risk, such as regions approaching stall or instability. These regimes demand cautious handling and generally contribute less to mission-level efficiency despite their local aerodynamic significance.

This weighting methodology enables the model to represent not only the aerodynamic performance of each AoA but also its functional importance, operational frequency, and safety implications within each climb phase. By integrating aerodynamic theory with practical mission dynamics, the proposed framework provides a more comprehensive and realistic evaluation of climb behaviour, consistent with methodologies adopted in previous studies [11, 31].

Table 3. Phase-specific angle of attacks (AoA) and weighting justification

Phase 1		
AoA (°)	**Description**	**Weight**
10	Initial acceleration	1.2
12	Critical CL generation	1.8
14	Peak lift	2
16	Stall limit, short duration	1

Phase 2		
AoA (°)	**Description**	**Weight**
8	Start of transition	1
10	Efficient lift/drag balance	2
12	Optimal value for climb	2.5
14	Upper limit, closely monitored	1.5

Phase 3		
AoA (°)	**Description**	**Weight**
6	Transition phase	1
8	Low drag, sufficient CL	2.5
10	Most efficient CL/CD point	3
12	Safe redundant climb	1.5

Phase 4		
AoA (°)	**Description**	**Weight**
4	High-speed start	1
6	Low AoA – CD minimization	2
8	Balanced transition	2
10	Pre-horizontal transition	1.5

3.3.2. Phase 1 (takeoff transition)

Figure 5 presents the CL, CD, and CL/CD performance of the original airfoils and their optimised variants within the angle of attack range of 10° to 16°. According to the results obtained for this phase, SG6042_Best demonstrates the highest lift performance, steadily increasing to nearly 1.76 at 16°, maintaining its superiority among all profiles. NLF1015_Best closely follows, reaching approximately 1.68. TL54_Best, while improved over its baseline version, still trails behind with a CL of around 1.61 at 16°. The trend confirms that SG6042-based profiles offer better lift characteristics under Phase 1 conditions.

Across the same AoA range, TL54_Best consistently shows the lowest drag, with CD values ranging from ~0.015 to just under 0.035. SG6042_Best exhibits a slightly higher drag profile but remains within acceptable bounds (0.01–0.04), especially given its superior lift output. NLF1015_Best, while delivering reasonable lift, produces noticeably more drag, particularly at higher AoA (above 14°), reaching over 0.06.

In terms of aerodynamic efficiency (CL/CD), TL54_Best is the clear leader, maintaining values from ~105 at 10° down to ~45 at 16°, showing both high performance and stability. SG6042_Best starts nearly as strong (~100 at 10°) but degrades faster, dropping to ~50 at 16°. In contrast, NLF1015_Best begins lower (~70) and shows the steepest decline, falling to just ~30 at 16°, indicating significantly lower efficiency at higher angles of attack.

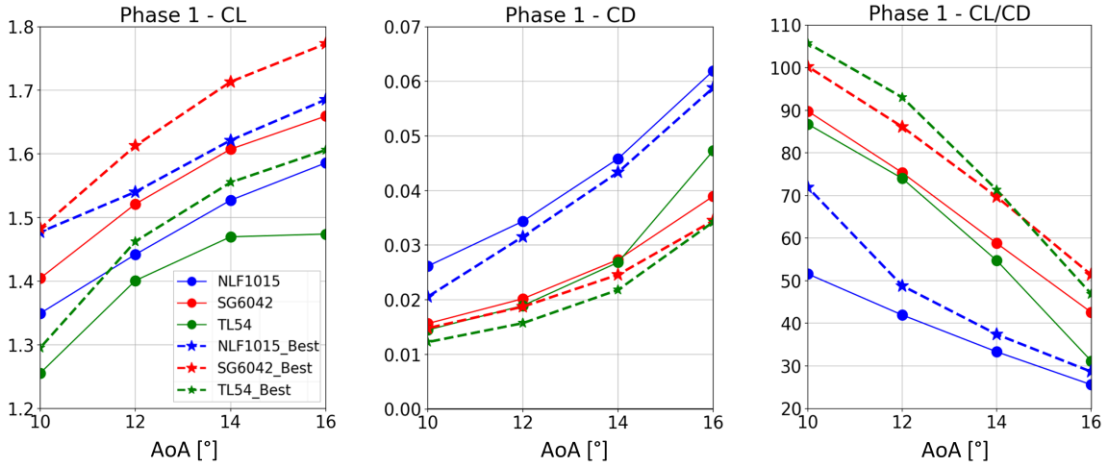

Figure 5. Phase 1 aerodynamic performance: lift, drag, and efficiency

In Phase 1, TL54_Best offers the best aerodynamic efficiency (highest CL/CD) due to consistently low drag, despite having the lowest lift. SG6042_Best provides the highest lift and balanced drag, making it a solid compromise, but not the most efficient. NLF1015_Best starts with decent lift, but increasing drag at higher AoA leads to significantly reduced efficiency.

3.3.3. Phase 2 (initial climb)

Figure 6 presents the CL, CD, and CL/CD performance of the original airfoils and their optimised variants within the relevant angle of attack range for Phase 2 (8° to 14°). In this intermediate AoA range, SG6042_Best leads in lift generation, reaching CL values above 1.7 at 14°, followed closely by NLF1015_Best, which approaches 1.65. TL54_Best, while showing noticeable improvement over its baseline, remains the lowest performer with a CL slightly above 1.5 at 14°. The data indicate that SG6042-based profiles are better suited for moderate lift demands encountered during the initial climb phase.

TL54_Best again demonstrates the lowest drag characteristics, with CD values consistently under 0.022. SG6042_Best follows with moderate drag (~0.013–0.025), offering a reasonable compromise between lift and drag. In contrast, NLF1015_Best continues to suffer from increased drag as AoA rises, reaching nearly 0.042 at 14°, indicating reduced aerodynamic cleanliness compared to the other profiles.

When efficiency is evaluated via CL/CD, TL54_Best surprisingly outperforms others across much of the AoA range, achieving values up to 115 at 8°, and remaining above 90 at 12°. Despite lower lift, its minimal drag enhances its efficiency. SG6042_Best maintains a strong performance (≈115–70), while NLF1015_Best shows a steeper decline, dropping to ~40 at 14°, signalling diminishing returns in efficiency.

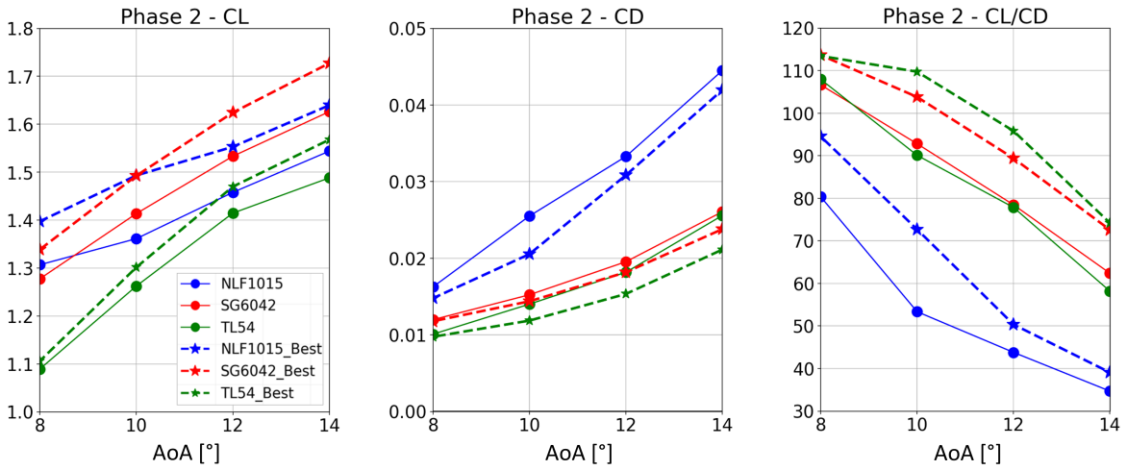

Figure 6. Phase 2 aerodynamic performance: lift, drag, and efficiency

During Phase 2, TL54_Best offers the best aerodynamic efficiency (highest CL/CD) owing to its consistently low drag, though its lower lift may be a limiting factor depending on climb demands. SG6042_Best delivers the highest lift and moderate drag, making it a solid all-around performer but not the most efficient. NLF1015_Best provides decent lift but is compromised by rising drag, resulting in the lowest overall efficiency across the evaluated AoA range.

3.3.4. Phase 3 (steady climb)

During Phase 3, which corresponds to steady climb conditions, the aerodynamic performance of both original and optimised airfoils, specifically CL, CD, and CL/CD, is illustrated in Figure 7 across the 6° to 12° angle of attack range. In this regime, SG6042_Best consistently achieves the highest lift (CL), peaking at ~1.66 at 12°, narrowly ahead of NLF1015_Best (~1.55). TL54_Best, while improved compared to its baseline, remains lower at ~1.47, indicating reduced lift capacity relative to the others. These results confirm SG6042_Best as a top performer in lift generation, though NLF1015_Best remains competitive in this aspect.

Drag performance in this phase is led by TL54_Best, maintaining the lowest CD values (≈0.008–0.015) across the AoA range. SG6042_Best follows with moderate drag values, generally staying below 0.02. Conversely, NLF1015 and its variant exhibit the highest drag growth with increasing AoA, reaching over 0.03 by 12°, marking a clear disadvantage in sustained climb efficiency.

Efficiency trends (CL/CD) reinforce the earlier observations. TL54_Best and SG6042_Best exhibit stable and high efficiency across the AoA range, peaking near 117 and 120 respectively at 6°–8°, and remaining above 90 at 12°. NLF1015_Best, despite an initial advantage at 6°, undergoes a rapid efficiency drop, falling to around 50 at the upper AoA limit. The divergence becomes pronounced from 8° onward, underscoring the reduced suitability of NLF1015_Best for sustained climb operations where consistent aerodynamic efficiency is essential.

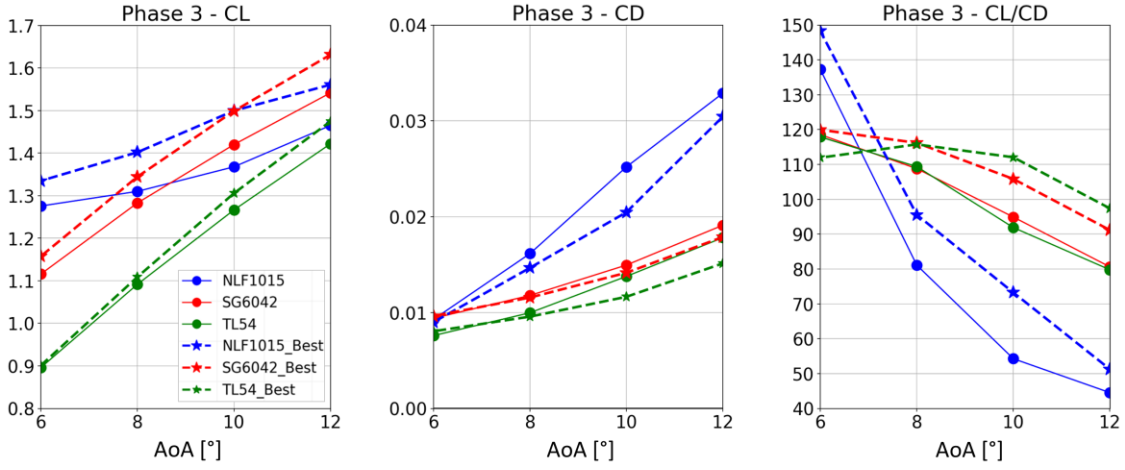

Figure 7. Phase 3 aerodynamic performance: lift, drag, and efficiency

In Phase 3, SG6042_Best presents the most balanced aerodynamic performance, offering a high lift coefficient (CL) and a competitive lift-to-drag ratio (CL/CD), particularly at higher angles of attack (AoA), making it the most well-rounded option. TL54_Best, despite having a lower maximum lift, consistently achieves the highest aerodynamic efficiency (CL/CD) across the AoA range due to its low drag (CD) characteristics, suggesting suitability for cruise or endurance-focused applications. On the other hand, NLF1015_Best, while generating moderate lift, suffers from substantially higher drag, which causes a sharp decline in its CL/CD performance as AoA increases, rendering it less favourable for sustained climb or efficient flight phases.

3.3.5. Phase 4 (pre-cruise levelling)

Figure 8 illustrates the lift, drag, and aerodynamic efficiency (CL, CD, and CL/CD) of the baseline and optimised airfoils during Phase 4, evaluated over the angle of attack range from 4° to 10°, representative of pre-cruise levelling conditions. In Phase 4, where lift requirements are moderate, SG6042_Best delivers the highest lift coefficient at higher angles of attack, reaching approximately 1.5 at 10° AoA, closely followed by NLF1015_Best. However, at lower AoAs, NLF1015_Best demonstrates superior lift performance, indicating its advantage in early stages of the angle of attack range. TL54_Best, although improved over its baseline, reaches a CL around 1.4, indicating slightly lower lift-generating capacity in this configuration.

From a drag perspective, TL54_Best consistently exhibits the lowest CD values compared to other best variants across the entire AoA range, from approximately 0.007 at 4° to just under 0.013 at 10°, making it the most aerodynamically efficient in terms of minimizing resistance. SG6042_Best shows marginally higher drag, peaking around 0.014 at 10°, while NLF1015_Best incurs the greatest penalty, with drag values rising significantly above 0.02 at 10°, especially after 6°, which compromises its overall efficiency in this phase.

The CL/CD plots further support these observations. SG6042_Best maintains stable and favourable aerodynamic efficiency, ranging between 108 and 122 across the AoA span. TL54_Best exhibits a strong mid-AoA performance, peaking slightly above 110 between 6° and 8°, demonstrating effective cruise-transition behaviour. NLF1015_Best, despite an exceptionally high initial efficiency of around 185 at 4°, experiences a steep and continuous decline, dropping to around 72 at 10°, confirming its diminishing returns at elevated angles and its reduced suitability for sustained moderate-angle flight.

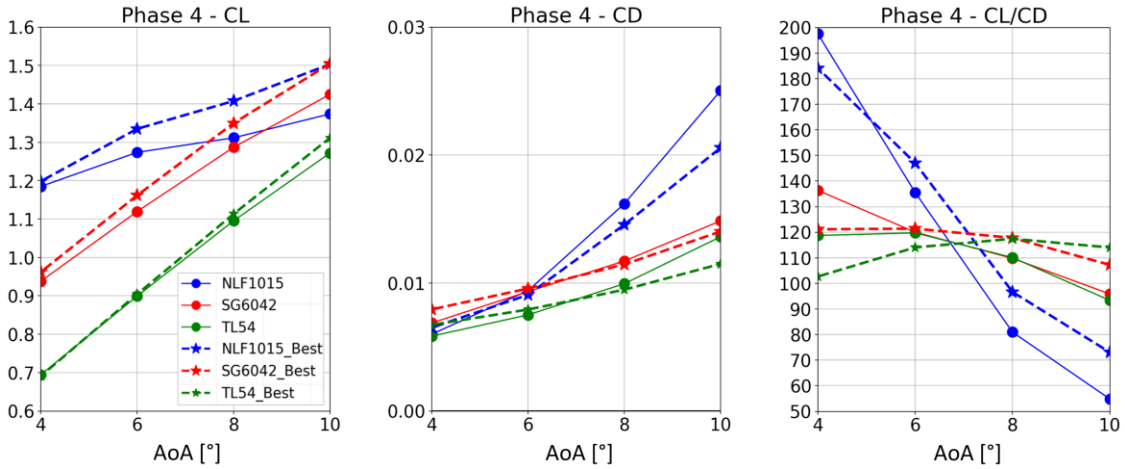

Figure 8. Phase 4 aerodynamic performance: lift, drag, and efficiency

In Phase 4, SG6042_Best again emerges as the most well-rounded airfoil, combining strong lift performance with stable aerodynamic efficiency (CL/CD ~110–130) and moderate drag levels, making it a robust candidate for pre-cruise flight conditions. TL54_Best, although limited in peak lift, demonstrates superior drag characteristics across the AoA range and maintains competitive efficiency, particularly in the AoA band (8–10°) where CL/CD exceeds 115. In contrast, NLF1015_Best, despite an initially high efficiency, shows a steep efficiency drop and increasing drag beyond 6°, rendering it less suitable for the sustained, moderate-to-high AoA operation typical of cruise preparation phases.

3.3.6. Complete climb phase

In this section, the complete climb phase is evaluated using a weighted average approach based on the total weights assigned to each angle of attack across all four phases (see Table 3), as illustrated in Table 4. The analysis was conducted under representative climb conditions, with an average Reynolds number of 1.64×10^6, Mach number of 0.0905, and freestream velocity of 31.1 m/s. This enables a consolidated aerodynamic assessment that reflects the relative contribution of each AoA to the overall climb profile.

Table 4. AoA and weight assignment for complete climb phase

AoA (°)	Phase 1	Phase 2	Phase 3	Phase 4	Total Weight	Normalized Weight
4	–	–	–	1	1	4.20%
6	–	–	1	2	3	12.50%
8	–	1	2.5	2	5.5	22.90%
10	1.2	2	3	1.5	7.7	32.10%
12	1.8	2.5	1.5	–	5.8	24.20%
14	2	1.5	–	–	3.5	14.60%
16	1	–	–	–	1	4.20%

The comparison of lift coefficients (see Figure 9) clearly demonstrates that all optimised ("Best") versions provide consistent improvement in lift performance across the examined angle of attack (AoA) range (4° to 16°). Among all profiles, SG6042_Best exhibits the highest lift values, reaching approximately CL = 1.8 at 16°, which is notably higher than its original form. NLF1015_Best also shows a meaningful increase, reaching CL ≈ 1.7, outperforming its baseline version by around 0.1–0.15 units across most AoA points.

TL54_Best, although clearly improved compared to the original TL54 (especially at higher AoA), still maintains the lowest overall CL values among the three optimised profiles. However, its lift curve trend remains linear and predictable, which may be advantageous in control-sensitive phases such as level flight or cruise transitions.

The results clearly indicate that the aerodynamic optimisation process successfully enhanced the lift performance of all three baseline airfoils. Among them, SG6042_Best exhibits the most significant improvement, particularly in the high-AoA regime (above 12°), where it achieves a markedly higher lift coefficient compared to its original counterpart and other best variant airfoils.

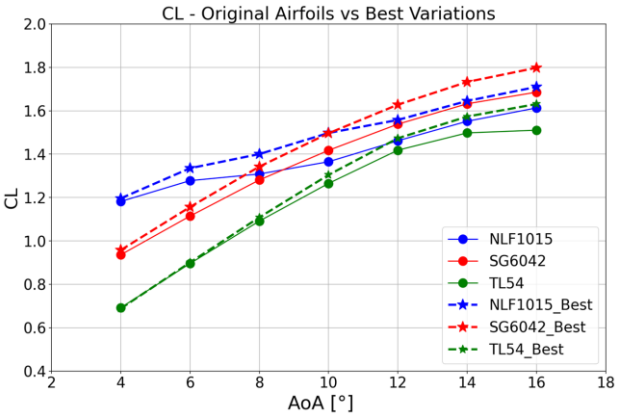

Figure 9. CL comparison of original and optimised airfoils across full climb AoA range

The CD results (see Figure 10) reveal a more nuanced picture. While all airfoils exhibit increasing drag with increasing AoA, as expected due to flow separation and pressure drag, the degree of increase varies significantly among the profiles. TL54_Best consistently maintains the lowest drag values, particularly in the mid-range AoA region (6°–14°), where CD remains under 0.025. This confirms the low-drag characteristics of airfoil, making it particularly suitable for cruise and steady climb conditions.

SG6042_Best performs well with respect to drag, showing values generally between 0.009 and 0.035 across the range. Importantly, its drag increase remains moderate even at higher AoA, which contributes significantly to its overall aerodynamic efficiency.

In contrast, NLF1015 and NLF1015_Best exhibit a steeper drag rise beyond 6°, with NLF1015_Best peaking around CD = 0.056 at 16°. This drag penalty, despite the associated lift gains, undermines its suitability in phases requiring energy efficiency or prolonged high-AoA operation.

The CD plot confirms that while optimising for lift is beneficial, it must be balanced with drag management to preserve overall efficiency, an area where SG6042_Best demonstrates a superior trade-off.

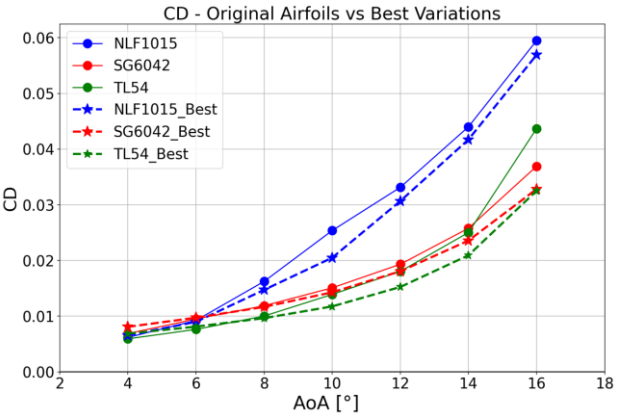

Figure 10. CD comparison of original and optimised airfoils across full climb AoA range

The CL/CD plot, representing aerodynamic efficiency, reinforces the combined interpretation of lift and drag trends (see Figure 11). SG6042_Best maintains the highest and most stable efficiency across most of the AoA spectrum. It begins with a CL/CD of about 120 at 4°, maintains over 100 up to 12°, and only drops to around 60 at 16°. This indicates strong performance both at low and moderate AoA, making it highly suitable for climb and cruise phases.

Interestingly, TL54_Best surpasses all others in the mid-AoA range (8°–14°), where its extremely low drag allows it to achieve CL/CD values around 75–120, despite slightly lower lift. This demonstrates that in flight regimes where drag minimization is critical, TL54_Best is a very efficient option, especially under conditions requiring sustained or economical performance.

On the other hand, NLF1015 and NLF1015_Best show rapid efficiency deterioration as AoA increases. Starting at very high CL/CD values (≈180–190 at 4°), their performance declines sharply, falling below 50 by 12°, and even lower by 16°. This confirms that NLF1015 variants are best suited for low-AoA applications, such as level cruise at lower incidence angles, but perform poorly at higher AoA due to increasing drag penalties.

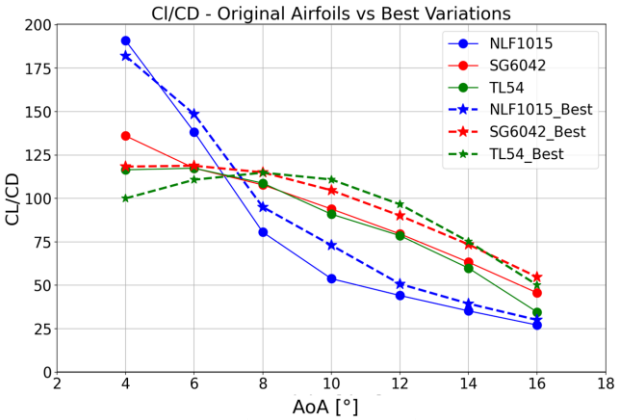

Figure 11. CL/CD comparison of original and optimised airfoils across full climb AoA range

The results clearly show that the optimized airfoils achieved CL performance improvements of up to 9.7%, 6.6%, and 7.9% compared to their conventional counterparts for the NLF1015, SG6042, and TL54 airfoils, respectively, across the entire angle of attack range. These findings are in good agreement with those reported in the literature [32, 33, 34].

The combined evaluation of lift, drag, and efficiency highlights clear distinctions among the airfoils:

- SG6042_Best offers the most balanced aerodynamic profile, with strong lift generation, moderate drag, and high efficiency across a wide AoA range. This makes it well-suited for multi-phase applications, including takeoff, climb, and cruise, particularly where performance uniformity and reliability are critical.
- TL54_Best shows specialised performance. It excels in drag reduction and maintains high efficiency, especially between 8°–14°, despite its lower lift. As such, it is highly appropriate for phases prioritizing drag minimization, such as steady climb or pre-cruise levelling. However, its use in high lift-demand situations (e.g., takeoff) would be limited.
- NLF1015_Best, while improved over its original form, exhibits performance volatility, especially in efficiency beyond mid-AoA. It could be beneficial in low-AoA regimes (e.g., level cruise) but is not recommended for higher AoA flight phases due to its poor drag characteristics.

From a design and optimisation perspective, this comparison illustrates the importance of tailoring airfoil selection to mission-specific flight phases. While some airfoils (like SG6042_Best) perform reliably across a broad range, others (like TL54_Best or NLF1015_Best) are better suited to narrow operational envelopes.

3.4. Climb Metrics and Energy Consumption

To analyse climb performances of each airfoil, such as climb rate, climb time, and energy consumption, it is first necessary to determine the primary forces acting on the aircraft. In this study, the weight force was approximated as a constant 1940 N, corresponding to an aircraft mass of roughly 198 kg [27]. This gravitational force is assumed to remain constant throughout all flight phases, as changes in total mass due to fuel or battery consumption are considered negligible.

In contrast, the required Thrust is not constant but varies significantly across the different stages of the climb to counteract aerodynamic drag. The thrust values for each phase were estimated based on the drag forces from reference UAV [27] based on the baseline airfoil, combined with the representative flight parameters of each segment. During the take-off transition, a thrust of approximately 485 N was required to overcome the high induced drag characteristic of low-speed flight. As the aircraft accelerated and gained altitude, the required thrust progressively decreased to 425 N in the initial climb, 357 N in the steady climb, and finally to 278 N during the pre-cruise levelling phase. This decreasing trend reflects the reduction in total drag, which is influenced by changes in both air density and lift coefficient as altitude and airspeed increase.

3.4.1. Climb performance analysis (rate and time)

This section presents a detailed evaluation of the climb performance characteristics, specifically climb rate and climb time, of the optimised airfoil variants compare to their original profiles across the four defined flight phases. The analysis aims to quantify the practical benefits of aerodynamic refinement by examining how improvements in lift, drag, and overall efficiency translate into mission-relevant performance metrics. Results are assessed phase-by-phase, providing insight into how each optimised airfoil performs under varying aerodynamic demands throughout the climb envelope.

To quantify the impact of airfoil modifications on flight performance, a quasi-steady climb model was implemented. This model evaluates key metrics, including the rate of climb and time to climb using the weighted average lift-to-drag ratio (CL/CD) as the primary aerodynamic input.

The Rate of Climb (RoC), defined as the vertical velocity of the aircraft, is determined using the excess power method. First, the total aerodynamic drag (D) is estimated under the assumption of a shallow climb angle, where lift (L) is approximately equal to the aircraft weight (W). The drag is therefore calculated using Eq.2:

$$D = \frac{W}{CL/CD} \tag{2}$$

The excess power (P_{ex}), which is the surplus power available to increase the aircraft's potential energy, is the difference between the power available from the propulsion system ($P_a = T \times V$) and the power required to overcome drag ($P_r = D \times V$). The RoC is then obtained by dividing the excess power by the aircraft weight as in Eq. 3:

$$RoC = \frac{P_{ex}}{W} = \frac{(T - D)V}{W} \tag{3}$$

where T represents the available thrust, V is the true airspeed in each phase, and W is the aircraft weight.
The time required to climb (t) a given altitude difference (Δh) is subsequently calculated by dividing the total altitude gain by the average rate of climb using Eq. 4:

$$t = \frac{\Delta h}{RoC} \tag{4}$$

In Phase 1, corresponding to the takeoff transition where angles of attack (AoA) are high (10°–16°), the effects of airfoil optimisation on climb performance are most pronounced (see Figure 12). All optimised ("Best") variants exhibit superior climb rates and reduced climb times relative to their baseline counterparts. TL54_Best achieves the highest climb rate (~5.35 m/s) and the greatest reduction in climb time (from ~38.0 s to 37.4 s). SG6042_Best follows closely, with a moderate improvement in both metrics, while NLF1015_Best shows a more modest increase in climb rate (from ~5.03 to 5.13 m/s) and a time reduction of approximately 0.7 s. These enhancements are primarily attributed to improvements in lift and the lift-to-drag ratio at elevated AoA.

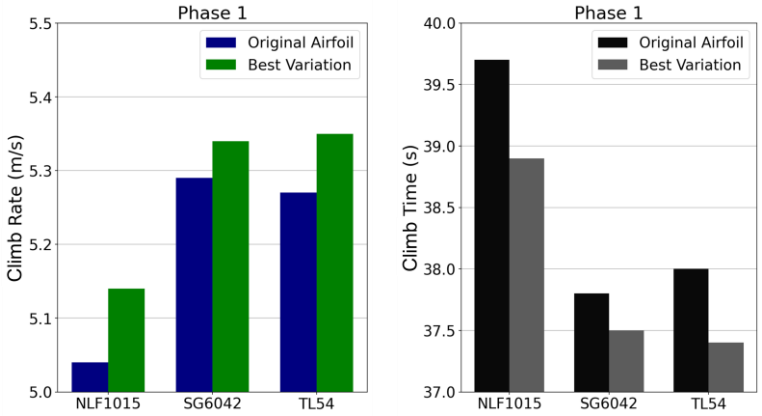

Figure 12. Climb rate and time comparison in Phase 1

In Phase 2 (see Figure 13), where AoA is reduced and aerodynamic efficiency becomes the dominant factor, SG6042_Best and TL54_Best continue to demonstrate superior performance, achieving climb rates of approximately 5.73–5.74 m/s and time reductions of 1.6 s and 1.0 s, respectively. The NLF1015_Best airfoil yields a smaller gain (~0.07 m/s increase in climb rate and ~0.7 s time reduction), limited by its higher drag levels in this AoA range.

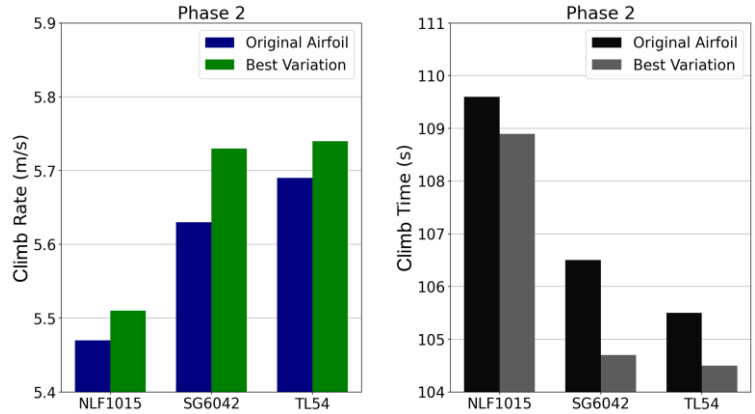

Figure 13. Climb rate and time comparison in Phase 2

During Phase 3 (see Figure 14), representing steady climb conditions (~6°–12° AoA), all optimised profiles maintain improved performance. SG6042_Best and TL54_Best exhibit similar climb rates (~5.68–5.69 m/s) and reduce climb times by ~0.6–0.7 s. Notably, NLF1015_Best shows a relatively larger improvement in this phase, decreasing its climb time from ~126.7 s to 125.0 s, although it remains the least efficient due to its persistent drag penalty.

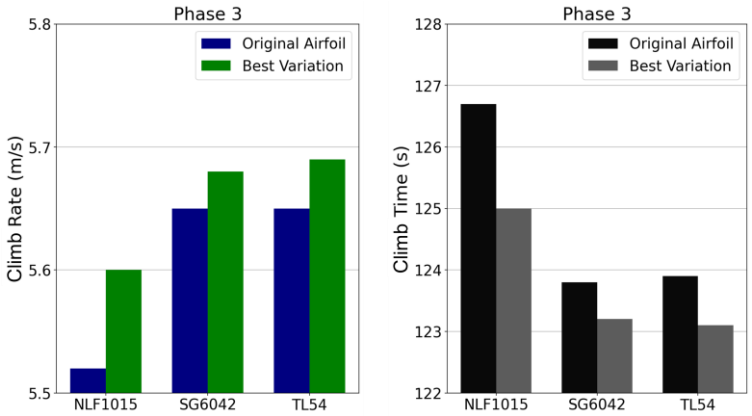

Figure 14. Climb rate and time comparison in Phase 3

In Phase 4 (see Figure 15), which corresponds to the final stage of climb with minimal AoA (~4°–10°), the performance differences diminish but remain consistent. All optimised variants show marginal climb rate improvements (~0.01–0.03 m/s) and small-time reductions. SG6042_Best and NLF1015_Best reach climb rates of 4.99 m/s, with time savings of ~0.2–0.6 s, while TL54_Best follows at 4.98 m/s. These gains are primarily attributed to reduced drag at low incidence angles, reaffirming the value of shape optimisation even under mild aerodynamic conditions.

Across all four climb phases, the optimised ("Best") airfoil variants consistently outperform their baseline counterparts in both climb rate and climb time, with the most significant improvements observed in Phases 1 through 3, where lift demand and aerodynamic efficiency are most influential. SG6042_Best demonstrates the most robust and consistent performance across all segments, achieving both high climb rates and the shortest climb times. This is attributed to its well-balanced aerodynamic profile, effectively combining strong lift generation with manageable drag. TL54_Best, while not matching SG6042_Best in lift production, compensates through exceptionally low drag characteristics, resulting in highly competitive climb rates and time reductions, particularly in phases where efficiency dominates. In contrast, NLF1015_Best, though improved through optimisation, remains limited in both metrics due to its sensitivity to drag growth at higher angles of attack. This limitation reduces its effectiveness during dynamic climb segments and suggests its aerodynamic characteristics are better suited to flatter, cruise-oriented flight conditions rather than sustained or aggressive ascent.

These climb rate and climb time outcomes align well with prior CL, CD, and CL/CD analyses, and confirm the practical aerodynamic advantage achieved through airfoil optimisation for mission-specific flight segments.

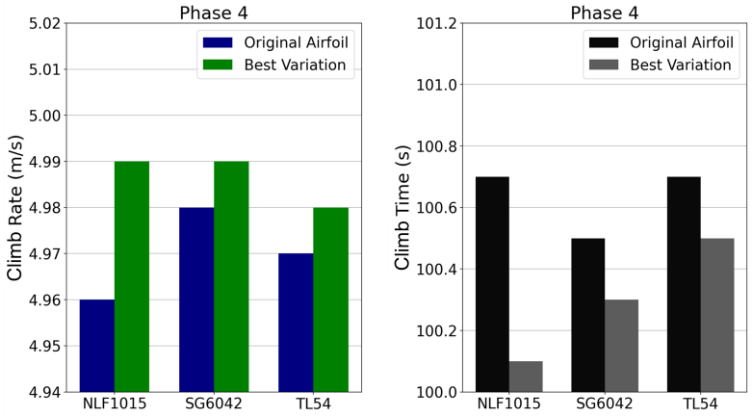

Figure 15. Climb rate and time comparison in Phase 4

The analysis of both climb rate and climb time across the complete climb envelope reinforces earlier aerodynamic evaluations and highlights the tangible benefits of airfoil optimisation, as shown in Figure 16. The results confirm that each optimised ("Best") variant provides measurable performance improvements over its baseline configuration, with system-level implications. Key findings include:

SG6042_Best:

- Provides the most consistent and well-rounded performance across all phases.
- Achieves high climb rates, owing to its well-balanced aerodynamic profile that combines strong lift generation with controlled drag.
- Demonstrates suitability for a wide range of flight conditions, from high-lift to low-drag regimes.

TL54_Best:

- While not the highest lift producer, it consistently benefits from exceptionally low drag, resulting in competitive climb rates and notable time reductions.
- Its aerodynamic efficiency makes it ideal for energy-conscious applications, such as long-endurance missions or high-efficiency cruise profiles.

NLF1015_Best:

- Shows modest improvements in both climb rate and time.
- Gains are constrained by significant drag sensitivity at higher angles of attack, limiting its effectiveness in sustained or steep climbs.
- Its performance characteristics suggest it is better suited to flatter cruise conditions rather than dynamic ascent segments.

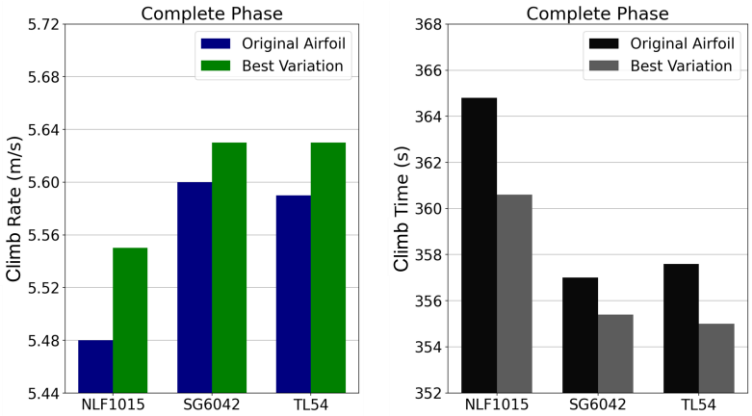

Figure 16. Overall climb performance summary: rate and time across all phases

3.4.2. Climb-phase energy consumption (Wh)

The total energy consumed (E) from the power source during the climb is determined in the present section. This calculation accounts for the total power output from the propulsor ($T \times V$), the duration of the climb (t), and the overall propulsive efficiency (η). The resulting energy in Watt-hours (E_{Wh}) is giving in Eq. 5:

$$E_{Wh} = \frac{(T \times V) \times t}{3600 \times \eta} \quad (5)$$

The division by 3600 converts the energy from the standard SI unit of Joules to the more common unit of Watt-hours. This model provides a consistent basis for comparing the energy efficiency of the baseline and optimised airfoil designs under identical flight conditions.

As shown in Equation (5), the total energy consumption of the UAV is directly influenced by its propulsive efficiency. Therefore, three different propulsive efficiency (η) levels (30%, 65%, and 80%) representing low, moderate, and high efficiency conditions were analysed in this study. Although the absolute energy consumption increases as propulsive efficiency decreases, the percentage difference between the baseline and optimized airfoils remains constant across all efficiency levels. The energy consumption for both baseline and optimized airfoils over the complete climb phase was computed assuming a propulsive efficiency of η = 0.65, as presented in Figure 17. The results clearly demonstrate that all three optimized airfoils (best variants) yield noticeable reductions in total energy usage. This finding confirms that aerodynamic refinement not only enhances flight dynamics but also translates directly into measurable operational efficiency improvements.

Among the profiles, NLF1015_Best shows the largest relative energy reduction, approximately 1.16%. This result is noteworthy, especially considering that NLF1015 was previously identified as the least favourable in terms of aerodynamic efficiency. The improvement in energy usage here likely stems from reductions in both drag and climb duration, despite the profile's less efficient high-AoA behaviour.

SG6042_Best continues to demonstrate its role as the most well-rounded and consistently high-performing profile. With an energy saving of 0.47%, it pairs superior aerodynamic balance (lift and drag) with minimal climb times, thus confirming its suitability for mission profiles where reliability, versatility, and energy optimization are all critical.

TL54_Best, previously highlighted for its exceptionally low drag characteristics, achieves a 0.72% energy saving, despite its relatively lower lift. This further confirms that, particularly in energy-constrained or electrically powered platforms, optimizing for minimum drag can be just as important as maximizing lift.

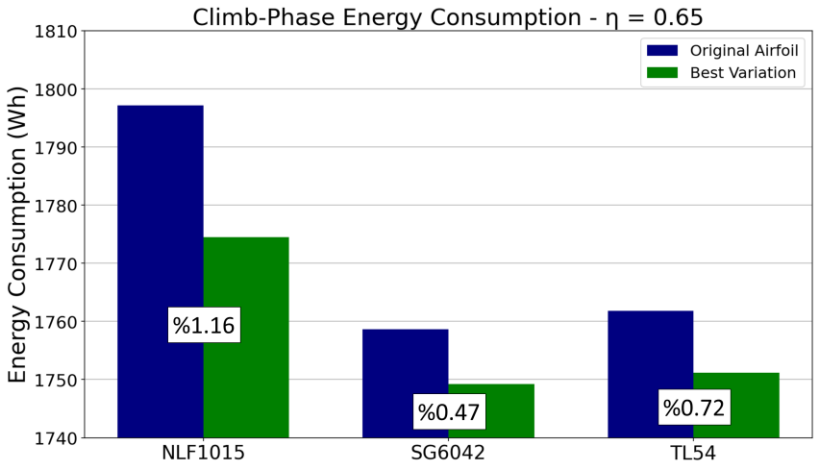

Figure 17. Comparison of climb-phase energy consumption for three airfoils and their optimized variations (η=0.65). percentages indicate energy savings

These trends align precisely with earlier observations regarding CL/CD behaviour and climb duration improvements. From this perspective, the findings support several actionable recommendations for airfoil selection and mission planning:

- SG6042_Best should be prioritized for general-purpose applications requiring balanced performance across all flight phases.
- TL54_Best is ideal for energy-limited missions, such as those involving battery-powered UAVs or solar-electric aircraft, where efficiency is paramount.
- NLF1015_Best, though improved, remains most suitable for low-AoA, cruise-dominant operations where its laminar flow characteristics can be fully exploited.

It seems these results could indicate that airfoil optimisation might lead to practical operational effects, rather than being solely a matter of theoretical aerodynamic advantage. Even small improvements in climb performance can yield meaningful advantages in:

- Fuel or energy efficiency,
- Total climb duration,
- Payload capacity and mission altitude,
- Overall flight endurance and mission throughput.

Therefore, selecting or designing airfoils tailored to mission-specific climb profiles can offer not just marginal improvements, but strategic aerodynamic advantages, particularly in UAVs and lightweight aircraft where performance margins are often limited.

3.5. Airfoil Recommendations

Based on a comprehensive analysis of aerodynamic performance, climb metrics, and energy use, the following recommendations are provided for mission-specific applications:

- SG6042_Best: Best All-Around Performer. This airfoil offers the most balanced profile, combining high lift with moderate drag. It is the top choice for missions prioritizing rapid ascent and strong overall climb capability, as it achieves the shortest time-to-altitude with reasonable energy efficiency.
- TL54_Best: Most Energy-Efficient. Excelling in drag minimization, this profile is ideal for energy-critical missions. It is highly recommended for applications like solar-powered or long-endurance electric UAVs, where minimizing power consumption is more important than achieving maximum lift.
- NLF1015_Best: Situational/Fallback Option. While improved from its baseline, this airfoil's high drag sensitivity in high-angle regimes makes it less optimal for demanding climbs. It is an acceptable choice for low-demand scenarios or when constrained by other design factors like manufacturing history.

These findings underscore the importance of aligning airfoil selection with specific mission objectives. A tailored aerodynamic design can lead to significant gains in flight performance, particularly for platforms where energy and time are operationally constrained.

4. CONCLUSION

This study definitively shows that mission-specific airfoil optimisation using CST geometry variation and XFOIL-based aerodynamic analysis provides tangible benefits for fixed-wing UAV climb performance. By evaluating and optimising three airfoil families (NLF1015, SG6042, TL54) across various climb phases, the research demonstrates how tailored aerodynamic improvements directly enhance climb rate, reduce climb time, and improve overall flight efficiency. Notably, SG6042_Best emerged as the most robust and balanced airfoil for rapid altitude gain missions due to its high lift and sustained efficiency, while TL54_Best excelled in minimizing drag, making it ideal for energy-conscious applications like solar-powered UAVs. Even marginal aerodynamic improvements yielded significant system-level impacts, translating into extended range, lower energy demands, and reduced operational costs. These findings underscore the critical importance of mission-phase specific airfoil

selection and optimisation, proving that informed aerodynamic tailoring, especially for climb-critical operations, unlocks substantial efficiency, performance, and reliability benefits at the mission level.

Limitations and Future Work

While the present study effectively demonstrates airfoil optimisation using CST and XFOIL for the rapid aerodynamic analysis of the baseline and variant profiles, it is inherently limited by several simplifying assumptions. These include XFOIL's constraints in modelling complex high-AoA aerodynamics, the 2D flow assumption neglecting critical 3D effects, and the exclusion of dynamic operational variables.

Future work should address these limitations by integrating high-fidelity CFD for critical flight phases and expanding to full 3D wing design. Exploring active drag reduction and multi-objective optimisation will further enhance prediction accuracy and align designs with real-world UAV mission requirements. Furthermore, future studies can be extended this framework using multi-objective optimizers such as NSGA-II to balance aerodynamic efficiency, energy use, and stability margins simultaneously.

Appendix A

Pseudocode summary of the airfoil optimisation workflow

```
# 1. Define base airfoil geometry
# ---------------------------------
# Either generate NACA 4-digit profile or import custom .dat file.
# Fit upper/lower surfaces using CST method with n coefficients.
# 2. Generate geometric variations
# ---------------------------------
# Create N variants by perturbing CST coefficients within a variation ratio.
# Apply Gaussian mask to emphasize leading/trailing edge fidelity.
# 3. Aerodynamic analysis via XFOIL
# ---------------------------------
for variant in airfoil_variants:
   for alpha in angle_of_attack_list:
      # Save .dat file
      # Run XFOIL for CL, CD, CM at given Re and Mach
      run_xfoil(variant, alpha, Re, Mach)
# 4. Performance evaluation
# -------------------------
for variant in all_variants:
   for alpha in angle_of_attack_list:
      cl_cd = get_cl_cd(variant, alpha)
      weighted_score += cl_cd * alpha_weights[alpha]
# Identify best-performing variant based on total weighted score
best_variant = variant_with_max_score()
# 5. Estimate climb performance
# -----------------------------
RoC = (T - W / L_D) / W * V        # vertical speed
t_climb = (h_end - h_start) / Roc   # climb time
Energy = ((T * V) * t_climb) / (3600 * propulsion_efficiency)  # energy consumption
# 6. Visualize results
# --------------------
plot_airfoil_shapes(original, best_variant)
plot_metrics_vs_alpha(['CL', 'CD', 'CM', 'CL/CD'])
plot_cp_distributions(original, best_variant, angle_of_attack_list)
```

Conflict of Interest

The author declares that there are no known competing financial interests or personal relationships that could have appeared to influence the work reported in this paper.

REFERENCES

[1] Santos PD, Gamboa P V. Evaluation of Energy Required for Flight by a UAV Fitted with a Variable-Span Wing Performing a Given Mission Profile. AIAA Atmospheric Flight Mechanics Conference.2015:1–9. https://doi.org/10.2514/6.2015-2391.

[2] Watanabe K, Shibata T, Ueba M. Derivation and Flight Test Validation of Maximum Rate of Climb during Takeoff for Fixed-Wing UAV Driven by Propeller Engine. Aerospace 2024;11. https://doi.org/10.3390/aerospace11030233.

[3] Suti A, Rito G Di, Galatolo R. Climbing performance enhancement of small fixed-wing UAVs via hybrid electric propulsion. Proc - 2021 IEEE Work Electr Mach Des Control Diagnosis, WEMDCD 2021 2021:305–10. https://doi.org/10.1109/WEMDCD51469.2021.9425638.

[4] Dündar Ö, Bilici M, Ünler T. Design and performance analyses of a fixed wing battery VTOL UAV. Eng Sci Technol an Int J 2020;23:1182–93. https://doi.org/10.1016/j.jestch.2020.02.002.

[5] Vale J, Lau F, Suleman A. Energy Efficiency Studies of A Morphing Unmanned Aircraft. J Aeronaut Aerosp Eng 2013;02. https://doi.org/10.4172/2168-9792.1000122.

[6] Kaneko S, Martins JR. Simultaneous optimization of design and takeoff trajectory for an eVTOL aircraft. Aerosp Sci Technol 2024;155:109617. https://doi.org/10.1016/j.ast.2024.109617.

[7] Gao Y, Qiao Z, Pei X, Wu G, Bai Y. Design of Energy-Management Strategy for Solar-Powered UAV. Sustainability. 2023;15(20):14972.

[8] Celik Y, Ingham D, Ma L, Pourkashanian M. Novel hybrid blade design and its impact on the overall and self-starting performance of a three-dimensional H-type Darrieus wind turbine. J Fluids Struct 2023;119:103876. https://doi.org/10.1016/j.jfluidstructs.2023.103876.

[9] Manolesos M, Celik Y, Ramsay H, Karande R, Wood B, Dinwoodie I, et al. Performance improvement of a Vestas V52 850kW wind turbine by retrofitting passive flow control devices. J Phys Conf Ser 2024;2767. https://doi.org/10.1088/1742-6596/2767/2/022027.

[10] Celik Y. A Comparative Aerodynamic Analysis of NACA and NREL Aerofoils for Darrieus Turbines Using CFD. Int J Innov Eng Appl 2022;6:111–7. https://doi.org/10.46460/ijiea.1075684.

[11] Rouco P, Orgeira-Crespo P, Rey González GD, Aguado-Agelet F. Airfoil Optimization and Analysis Using Global Sensitivity Analysis and Generative Design. Aerospace 2025;12. https://doi.org/10.3390/aerospace12030180.

[12] Hasan MS, Svorcan JM, Simonovic AM, Mirkov

NS, Kostic OP. Optımal Aırfoıl Desıgn And Wıng Analysıs For Solar-Powered Hıgh-Altıtude Platform Statıon. Explor Econ Hist 1993;24:ETG 5-1-ETG 5-17. https://doi.org/10.1080/00033799300200371.
[13] Nikolaou E, Kilimtzidis S, Kostopoulos V. Multi-Fidelity Surrogate-Assisted Aerodynamic Optimization of Aircraft Wings. Aerospace 2025;12. https://doi.org/10.3390/aerospace12040359.
[14] Benaouali A, Kachel S. Multidisciplinary design optimization of aircraft wing using commercial software integration. Aerosp Sci Technol 2019;92:766–76. https://doi.org/10.1016/j.ast.2019.06.040.
[15] Kulfan BM, Bussoletti JE. "Fundamental" parametric geometry representations for aircraft component shapes. Collect Tech Pap - 11th AIAA/ISSMO Multidiscip Anal Optim Conf 2006;1:547–91. https://doi.org/10.2514/6.2006-6948.
[16] Masters DA, Taylor NJ, Rendall TCS, Allen CB, Poole DJ. Geometric comparison of aerofoil shape parameterization methods. AIAA J 2017;55:1575–89. https://doi.org/10.2514/1.J054943.
[17] Anitha D, Shamili GK, Ravi Kumar P, Sabari Vihar R. Air foil Shape Optimization Using Cfd and Parametrization Methods. Mater Today Proc 2018;5:5364–73. https://doi.org/10.1016/j.matpr.2017.12.122.
[18] Guan X, Li Z, Song B. A study on CST aerodynamic shape parameterization method. Acta Aeronaut Astronaut Sin 2012;33(4):625–33.
[19] Straathof MH. Parametric study of the class-shape-refinement-transformation method. Optimization 2012;61:637–59. https://doi.org/10.1080/02331934.2011.627335.
[20] Kulfan BM. Modification of CST airfoil representation methodology. [Internet] Http//Www Brendakulfan Com/Docs/CST8 Pdf 2009;7:21.
[21] Zhu F, Qin N. Intuitive class/shape function parameterization for airfoils. AIAA J 2014;52:17–25. [cited 2025 December 12] https://doi.org/10.2514/1.J052610.
[22] Olson ED. Three-dimensional piecewise-continuous class-shape transformation of wings. 16th AIAA/ISSMO Multidiscip Anal Optim Conf 2015:1–16. https://doi.org/10.2514/6.2015-3238.
[23] Su H, Gong CL, Gu LX. Two-level aerodynamic shape optimization strategy based on three-dimensional CST modeling method. J Solid Rocket Technol 2014;37(1):1–6.
[24] Mark D. XFOIL: An analysis and design system for low Reynolds number airfoils. Low Reynolds Number Aerodyn. Springer, 1989, p. 1–12.
[25] Singh AP; Winoto SH; Shah DA; Lim KG; Goh RE. A computational study on airfoils at a low Reynolds number. ASME Int Mech Eng Congr Expo 2000;19258:405–11.
[26] Arshad A, Rodrigues LB, López IM. Design Optimization and Investigation of Aerodynamic Characteristics of Low Reynolds Number Airfoils. Int J Aeronaut Sp Sci 2021;22:751–64. https://doi.org/10.1007/s42405-021-00362-2.
[27] Panagiotou P, Yakinthos K. Aerodynamic efficiency and performance enhancement of fixed-wing UAVs. Aerosp Sci Technol 2020;99:105575. https://doi.org/10.1016/j.ast.2019.105575.
[28] Kimmons J; Thomas P; Colonia S. Aerodynamic effects of surface deformities on aerofoils for low-speed stratospheric flight. Proc Inst Mech Eng Part G J Aerosp Eng 2023;237(1):108–29.
[29] Durmus S. Aerodynamıc Performance Comparıson Of Aırfoıls In Flyıng Wıng UAV. Journal, Int Appl Innov Eng 2023;7.
[30] Ceze M, Hayashiy M, Volpez E. A study of the CST parameterization characteristics. Collect Tech Pap - AIAA Appl Aerodyn Conf 2009. https://doi.org/10.2514/6.2009-3767.
[31] Sasaki D, Ito A, Ishida T, Nakahashi K. Design optimization of a mild-stall airfoil/wing for UAV and PAV applications. Collect Tech Pap - AIAA Appl Aerodyn Conf 2009:1–15. https://doi.org/10.2514/6.2009-4111.
[32] Carreño Ruiz M, Renzulli L, D'Ambrosio D. Airfoil optimization for rotors operating in the ultra-low Reynolds number regime. Phys Fluids 2023;35. https://doi.org/10.1063/5.0166170.
[33] Hansen TH. Airfoil optimization for wind turbine application. Wind Energy 2018;21:502–14. https://doi.org/10.1002/we.2174.
[34] Liang C, Xi D, Zhang S, Chen B, Wang X, Guo Q. Optimization on Airfoil of Vertical Axis Wind Turbine Based on CST Parameterization and NSGA-II Aigorithm 2016:1–17. https://doi.org/10.20944/preprints201608.013.